Food Chemistry: X 14 (2022) 100314

Contents lists available at ScienceDirect

Food Chemistry: X

journal homepage: www.sciencedirect.com/journal/food-chemistry-x

Structural characterization and hypolipidemic activity of *Gracilaria lemaneiformis* polysaccharide and its degradation products

Xiaoshan Long [a,b], Xiao Hu [b,c,d], Huan Xiang [b], Shengjun Chen [b], Laihao Li [b], Bo Qi [b], Chunsheng Li [b], Shucheng Liu [a,d,*], Xianqing Yang [b,c,d,*]

[a] College of Food Science and Technology, Guangdong Ocean University, Guangdong Provincial Key Laboratory of Aquatic Products Processing and Safety, Guangdong Provincial Engineering Technology Research Center of Marine Food, Guangdong Province Engineering Laboratory for Marine Biological Products, Zhanjiang 524088, China

[b] Key Laboratory of Aquatic Product Processing, Ministry of Agriculture and Rural, South China Sea Fisheries Research Institute, Chinese Academy of Fishery Sciences, Guangzhou 510300, China

[c] Co-Innovation Center of Jiangsu Marine Bio-Industry Technology, Jiangsu Ocean University, Lianyungang 222005, China

[d] Collaborative Innovation Center of Seafood Deep Processing, Dalian Polytechnic University, Dalian 116034, China

ARTICLE INFO

Keywords:
G. *lemaneiformis*
Polysaccharide
Structural characterization
Hypolipidemic activity
Pancreatic lipase
Cholesterol esterase

ABSTRACT

This research aimed to analyze structural characterization and hypolipidemic activity *in vitro* of G. *lemaneiformis* polysaccharide (GLP) and its degradation products. The results presented that the content of galacturonic acid declined and glucuronic acid level enhanced, average particle size decreased from 99.9 μm to 25.7 μm, and color brightness of polysaccharide strengthened after degraded by H_2O_2-Vc. There was no significant change in thermal stability of polysaccharide before and after degradation. It was observed in AFM analysis, polysaccharide changed to smaller, delicacy and dispersion after degradation. As seen in FT-IR, H_2O_2-Vc degradation never change the structure of polysaccharide. Polysaccharide and its degradation products showed a significant inhibition effect on pancreatic lipase and cholesterol esterase in a dose-dependent manner, which presented the mixed type of competitive and non-competitive for pancreatic lipase, and non-competitive for cholesterol esterase, respectively. The fluorescence quenching type was static on pancreatic lipase and dynamic on cholesterol esterase.

1. Introduction

Pancreatic lipase and cholesterol esterase exhibit the ability to hydrolyze fat and promote absorption of dietary fat in gastrointestinal tract, which has therapeutic and preventive effects on hyperlipidemia (Li et al., 2021). Pancreatic lipase is mainly secreted by pancreatic acinar and stomach cells, which is the most important enzyme in the hydrolysis of dietary fat. It can hydrolyze triglyceride and cholesterol into glycerol monoesters and fatty acids, which are absorbed by small intestinal epithelial cells (Zhang et al., 2019). While cholesterol esterase is a non-specific serine hydrolase, mainly from pancreas and mammary gland of higher mammals (Aggarwal, Malik, Prashant, Jaiwal, & Pundir, 2016; Zhao, Wu, & Hu, 2021). It has been found that cholesterol esterase performs a critical role in transporting free cholesterol from micelles to enterocytes (Boyd et al., 2021; Zhao, Wu, & Hu 2021). In addition, cholesterol esterase also plays an essential role in industry, as biosensors, paper degradants, catalysts and additives (Aggarwal et al., 2016; Singh, Chaubey, & Malhotra, 2004; Yasutake et al., 2021). Increasing evidence has investigated the inhibition effect of polysaccharide on pancreatic lipase and cholesterol esterase *via* inhibition rate, inhibition kinetics and fluorescence quenching (Huang et al., 2020). For example, Zhang, Wu, Wei, and Qin (2020) attained the inhibition action of *Camellia nitidissima* Chi against cholesterol esterase from the IC_{50} value, inhibition kinetics and fluorescence quenching. The results showed that the IC_{50} value of compounds A1H3 and A2H3 were 0.36 μM and 3.82 μM, and performed a mixed type inhibition and dynamic fluorescence quenching type. Heng et al. (2011) reported that the IC_{50} value was 5.89 μM and mixed-type inhibition occurred on cholesterol esterase from rhodanine and thiazolidinedione scaffolds. Generally speaking, these indicators, including inhibition rate, inhibition kinetics and fluorescence quenching, are able to reflect the inhibition effect on pancreatic lipase and cholesterol esterase.

* Corresponding authors at: Collaborative Innovation Center of Seafood Deep Processing, Dalian Polytechnic University, Dalian 116034, China.
E-mail addresses: Lsc771017@163.com (S. Liu), 1157440148@qq.com, yxqgd@163.com (X. Yang).

https://doi.org/10.1016/j.fochx.2022.100314
Received 26 January 2022; Received in revised form 24 February 2022; Accepted 18 April 2022
Available online 20 April 2022

Orlistat is an effective hypolipidemic drug, which owns a good inhibitory effect on pancreatic lipase and cholesterol esterase, but it also brings different degrees of side effects to the body, which is not conducive to long-term use. Therefore, the exploration of natural and no side effects of lipid-lowering drugs has become the focus of current research. Studies have found that polysaccharide, flavonoid, polyphenol and other active substances from algae and plants have significant inhibitory effects on pancreatic lipase and cholesterol esterase, showing an excellent effect of lowering blood lipid (Huang et al, 2020; Li et al., 2021; Siegien et al, 2021). It has been proved that *Ulva prolifera* polysaccharide weakened the activity of pancreatic lipase, presenting the anti-hyperlipidemia activity (Yuan et al., 2018). Godard et al. (2009) demonstrated that polysaccharide from the green alga ameliorated serum lipid profile of mice, declining its plasma cholesterol, non-HDL cholesterol and triglycerides. Research on the biological activity of algae and plants, and the development of products for adjuvant treatment of diseases, has become a current hot spot.

G. *lemaneiformis* is a kind of economic red algae, rich in polysaccharide, phycobiliprotein, pigment, mineral and other nutrients and active components, which plays essential roles in hypoglycemic, hypolipidemic, anti-bacteria, anti-cancer and other physiological activities (Chen, Xie, Yang, Liao, & Yu 2010; Chen et al., 2021; Fan, Wang, Song, Chen, Teng, & Liu, 2012; Huang et al., 2019; Huang et al., 2020; Long et al., 2021a; Sun et al., 2018; Wang et al., 2019). Li et al. (2020) revealed that G. *lemaneiformis* polysaccharide observably regulated the lipid metabolism and accelerated free fatty acid oxidation. According to previous reports, polysaccharide exhibits better physiological activities after degradation (Chen et al., 2020; Gong et al., 2021; Zhang et al., 2020). H_2O_2-Vc degradation is effectively to attain polysaccharide with lower molecular weight and high activities (Zhang, Wang, Zhao, & Qi, 2014). The degradation method of H_2O_2-Vc belongs to chemical degradation, promoted the breakage of glyosidic bonds by free radicals produced from H_2O_2-Vc (Shen et al., 2019; Yan et al., 2021). It is reported that H_2O_2 cuts the glyosidic bonds through hydroxyl groups, shortening the sugar chain of polysaccharide and thus reducing its molecular weight (Chen et al., 2021). Moreover, vitamins C (Vc) facilitates this process by reinforcing H_2O_2 to produce hydroxyl groups (Yan et al, 2021). The polysaccharide of G. *lemaneiformis* treated by H_2O_2-Vc showed the best hypoglycemic activity *in vitro*, and the molecular weight became lower and reducing sugar reinforced after degradation, compared with polysaccharide (Long et al, 2021b). In addition, polysaccharide manifested the better antioxidant and anti-tumor activities after degraded by H_2O_2-Vc, reported by Chen et al. (2020) and Shen et al. (2019), respectively.

The changes of structure and hypolipidemic activity *in vitro* of polysaccharide after degradation, as well as their relationship, are the scientific questions to be explored in this experiment. To resolve these scientific questions, this passage analyzed the changes of structural characteristics of polysaccharide before and after degradation, such as uronic acid content, particle size, X-Ray Diffraction (XRD), morphology features, and functional groups. Meanwhile, the inhibitory effects of polysaccharide and its degradation products on pancreatic lipase and cholesterol esterase were dissected *via* the indexes of inhibition rate, enzyme kinetics and fluorescence quenching.

2. Materials and methods

2.1. Materials and chemicals

G. *lemaneiformis* was purchased from Nan'ao Island (Shantou, Guangdong, China). Cholesterol esterase (CAS 9026-00-0) was purchased from Shanghai Yuanye Biotechnology Co., LTD, and pancreatic lipase (CAS 53608-75-6) was purchased from Aladdin Reagent (Shanghai) Co., LTD (Shanghai, China), 4-nitrophenylbutyrate (named PNPB, CAS 2635-84-9) was purchased from Hefei BoMei Biotechnology Co.Ltd (Hefei, China).

2.2. Preparation of GLP and its degradation products

The extraction method of GLP was referred to previous study. G. *lemaneiformis* was cleaned, dried, crushed and sifted through 40 mesh to obtain uniform powder. The powder was added 95% ethanol to remove pigment, fat and alcohol-soluble impurities for 24 h, and then dried at 50 ℃. After 30 min of ultrasonic wall breaking, G. *lemaneiformis* powder was extracted with water at a ratio of 1:45 (w/v) at 90 ℃ for 4 h with oscillating, and then cooled to room temperature to add 1% papain and 0.5% cellulase (W/V). The mixture was incubated at 60 °C for 2 h with oscillating, and then rapidly heated in boiling water for 10 min to denature the papain and cellulase. The mixture was centrifuged, and the supernatant was concentrated with rotary evaporation (60 ℃). The concentrated solution was precipitated, dialyzed (7 kDa) and freeze-drying. Then GLP was obtained (Long et al, 2021b).

GLP was degraded by H_2O_2-Vc (mole ratio of H_2O_2 and Vc was 1:1). In brief, GLP (5 mg/mL) and 18.7 mM of H_2O_2-Vc reacted at 56 ℃ for 0.5 h according to previous research (Long et al, 2021b). The degradation reaction was terminated by adjusting pH to neutral. Degradation product was added with anhydrous ethanol (four times the volume of the solution) and placed overnight at 4 ℃. After centrifugation, the supernatant was removed, and precipitation was redissolved to dialysis (300 Da) and lyophilized. The degradation product was obtained, named GLP-HV (G. *lemaneiformis* polysaccharide degraded by H_2O_2-Vc). Only H_2O_2 in the same concentration was used for polysaccharide, the other conditions were the same, the sample was obtained, named GLP-H (GLP degraded by H_2O_2). Only Vc in the same concentration was used for polysaccharide, the other conditions were the same, the sample was obtained, named GLP-V (GLP degraded by Vc). GLP-H and GLP-V were the controls of GLP-HV.

2.3. The yield of GLP and the content of galacturonic acid and glucuronic acid

Extraction rate was referred to the mass ratio of lyophilized polysaccharide to raw material. The content of galacturonic acid and glucuronic acid were detected by high performance liquid (HPLC) (Long et al, 2021b).

2.4. Particle size of GLP and its degradation products

The particle size of the samples was determined by Mastersizer 2000 (Malvern, England), and the determination results included D_{90}, D_{50}, D_{10} and Span. The determination results were repeated more than 3 times until the results were stable.

2.5. Color analysis of GLP and its degradation products

The color of the samples were determined by automatic chromaticity meter CR-400 (Konica Minolta, Japan), in which the color was expressed by L, a* and b*, and the color difference was expressed by △E. The L value (Lightness) varies from 0 to 100, where 0 represents black and 100 represents white. The value of a* (redness) is from red to green: 100 for red and −80 for green. b* (yellowness) symbolizes value from yellow to blue: 100 for yellow and −80 for blue. △E value refers to the total chromatic aberration.

2.6. XRD determination of GLP and its degradation products

XRD measurement of GLP, GLP-HV, GLP-H, and GLP-V samples were carried out using D8 ADVANCE diffractometer (BRUCKER, Germany) with Cu Kα tube in the 2 theta range of 2°–50° at scanning rate of 1.2°/min. The determination method was referred to literature with a few modifications (Bozoglan, Duman, & Tunc, 2020).

2.7. Thermal stability analysis of GLP and its degradation products

The samples of 5 mg were detected by STA 449F3 (Netzsch, Germany) from 50 to 900 ℃ at scanning rate of 10 ℃/min. This method was performed with modification (Nawrocka, Chargot, Miś, Wilczewska, & Markiewicz, 2017).

2.8. Atomic force microscope (AFM) analysis of GLP and its degradation products

The samples were dispersed and dripped onto mica for natural drying, and then tested in an intelligent imaging mode (Brucker AXS, Germany). The AFM analysis of GLP, were Dimension Icon (NanoScope Analysis 1.8) (Gong et al, 2021).

2.9. Fourier transform infrared spectroscopy (FT-IR) analysis

An appropriate amount of GLP, GLP-HV, GLP-H and GLP-V powders were mixed with KBr, respectively (dried for 12 h at 100 °C), then ground to uniform fine powder. The powders were pressed into transparent flakes, and infrared scanning was carried out in the wave number range of 4000–400 cm^{-1}, and KBr was as blank correction background. The FT-IR spectra of polysaccharide and their degradation products were measured and recorded (Wang et al, 2021).

2.10. Inhibitory effect of GLP and its degradation products on pancreatic lipase and cholesterol esterase

The inhibition effect on pancreatic lipase and cholesterol esterase referred to the literature with a few modifications (Siow, Choi, & Gan, 2016). The detailed experimental method was as follows: 50 μL different concentration of samples (1, 2.5, 5, 7.5, 10 mg/mL) mixed with 50 μL buffered solution (0.1 M, pH 8.0 of Tris-Hcl solution for pancreatic lipase, and 0.1 M, PH 7.0 of sodium bezoar cholate-sodium chloride solution for cholesterol esterase) and 50 μL enzyme (1 mg/mL pancreatic lipase or 5 U/mL cholesterol esterase) in 96-well plates, which incubated at 37 °C for 15 min, and added 100 μL 2 mg/mL PNPB solution. Then texted the absorbance value at 405 nm after reacting at 37 °C for 20 min under dark condition, and inhibition rate was calculated *via* formula (1).

The inhibition kinetics method was as follows: The samples' concentrations were 0, 1, and 5 mg/mL, and the concentration of PNPB was 0.25, 0.5, 1, 1.5, and 2 mM, respectively. The mix was reacted for 20 min, and the determination was measured every 2 min. *Lineweaver-Burk* curve was described by double reciprocal plotting method with reciprocal of substrate concentration as abscissa and reciprocal of reaction rate as ordinate (Huang et al, 2020), which calculated the Michaelis constant (*K*m) and the maximum reaction rate (*V*max) through formula (2).

Fluorescence spectrum analysis referred to Wang et al. (2022) with a few modifications. The excitation wavelength was 280 nm, the emission wavelength was from 290 to 500 nm, and the slit width was 5 nm. Samples solution (0.5 mL, 5 mg/mL) and 2.5 mL enzyme (1 mg/mL pancreatic lipase or 5 U/mL cholesterol esterase) were taken, and the fluorescence spectrum was measured under these conditions after shaking and mixing, and the samples were replaced by buffered solution as blank. The samples with the best activity were prepared with concentrations of 1, 2.5, 5, 7.5 and 10 mg/mL, and the fluorescence spectra was determined under the same conditions. The equations of *Stern-Volmer* (formulas (3)-(6)) were used to reflect the fluorescence quenching. All the formulas are as follows:

$$\text{Inhibition rate}/\% = \frac{(A_3 - A_4) - (A_1 - A_2)}{(A_3 - A_4)} \times 100, \quad (1)$$

$$\frac{1}{v} = \frac{1}{Vmax} + \frac{Km}{Vmax} \times \frac{1}{[S]} \quad (2)$$

$$\frac{F_0}{F} = 1 + K_{sv}[Q] = 1 + K_q \tau_0 [Q] \quad (3)$$

$$\frac{F_0}{F} = e^{K_{sv}[Q]} \quad (4)$$

$$K_{sv} = K_q \tau_0 \quad (5)$$

$$\lg\left(\frac{F_0 - F}{F}\right) = \lg K_a + n \lg[Q] \quad (6)$$

A_1: samples and enzyme; A_2: enzyme was replaced by buffered solution; A_3: samples were replaced with pure water; A_4: samples and enzyme were replaced with pure water and buffered solution, respectively.

V: initial reaction rate; *V*max: the maximum reaction rate; [S]: the concentration of PNPB; *K*m: the Michaelis constant.

F_0: fluorescence intensity of enzyme without samples; F: fluorescence intensity of enzyme with samples; [Q]: the concentration of samples; τ_0: the average life of fluorescent substances without quenching agent is generally 10^{-8}; K_q: quenching rate constant; K_{sv}: quenching constant of *Stern-Volmer*; K_a: the binding constant between samples and enzyme; n: the binding-site number.

3. Results and discussion

Chemical compositions

The yield of polysaccharide from G. *lemaneiformis* was 35.25% ± 2.403, which was higher than extracted by citric acid (22.8%) (Li et al., 2020) and enzyme extraction (16.8%) (Chen et al., 2020), and similar to Zhang et al. (2020) (34.84% by water extraction). Compared with other extraction methods, the water extraction and alcohol precipitation method in this study could obtain higher extraction rate of polysaccharide, illustrating that the extraction method was suitable to produce the polysaccharide. The galacturonic acid of GLP, GLP-HV, GLP-H, and GLP-V were 0.274%, 0.091%, 0.114%, and 0.094%, respectively. In addition, the glucuronic acid level of these four samples were 0.187%, 0.317%, 0.291%, 0.249%, severally. The content of these two uronic acids in polysaccharide and its degradation products were low, which may belong to neutral polysaccharide (Bettler, Amadò, & Neukom, 1990; Zhang, Yun, Zhang, & Liang, 2016). Degradation with H_2O_2 or Vc reduced the content of galacturonic acid and enhanced the glucuronic acid level. Especially when H_2O_2 and Vc were degraded together, the changes of these two uronic acids were most obvious ($p < 0.05$). The possible mechanism was that degradation caused the carboxyl group on galactose of polysaccharide to be replaced by other groups, while the primary hydroxyl group on glucose was converted to carboxyl group (Bendiak, Salyan, & Pantoja, 1994). The total uronic acid was reduced after degrade degradation by UV/H_2O_2, researched by Chen et al. (2021), which was similar to our study.

3.2. Particle size

The influence of degradation on the particle size of polysaccharide and its degradation products was analyzed in Table 1. Dn indicates that n% of the particle size is smaller than the value that D_{50} represents the average particle size. Span is on behalf of the particle size dispersion, and the particle size distribution is more concentrated when the value is small (Wiacek, & Stasiak, 2018). As shown in Table 1, the average particle size of polysaccharide decreased significantly after degradation ($p < 0.05$), and the D_{50} value of GLP-HV was 85.14 μm which emerged the best degradation effect of H_2O_2-Vc. There was no significant difference between the D_{50} values of GLP-H and GLP-V, and the average

particle size of the three degradation products were smaller than that of GLP ($p < 0.05$), illustrating the effective degradation. The D_{90} values of GLP-HV, GLP-H, and GLP-V were 224.74, 247.55, 283.86 μm, respectively, which were markedly lower than GLP ($p < 0.05$). These results explained that GLP-HV had the smallest particle size and the most delicate powder. The damage of H_2O_2-Vc on glyosidic bonds was more sufficient, resulting in more glyosidic bond breaks, causing shorter sugar chains and smaller molecules, promoting the decrease in average particle size. However, GLP-HV performed the largest Span value, while GLP-H expressed the smallest Span value ($p < 0.05$). It stated that the size of the polysaccharide obtained by H_2O_2-Vc degradation may be slightly obvious, resulting in diffusion and dispersion of distribution, compared with the degradation of H_2O_2 or Vc alone. But overall, the GLP-HV powder was the most delicate. The smaller particle size may perform the better activities because the surface area of interactions between molecules increased.

3.3. Color analysis

The influence of different degradation methods on the color of polysaccharide and its degradation products were compared, mainly represented by L, a*, b*, △E (Wiacek and Stasiak, 2018). The value of L means brightness, and the greater value leads to the stronger brightness. The a* represents the color change from green (−a) to red (+a), and the color shifts to red degree as the value becomes bigger. The b* indicates that the color changes from blue (−b) to yellow (+b), and the color moves towards yellow degree with increasing value. △E is the value of color difference. As can be seen from Table 2, after the polysaccharide was degraded by H_2O_2-Vc, the brightness of GLP-HV (87.17) increased distinctly and shifted to green and yellow, compared to GLP (the brightness was 74.61). The brightness of GLP-H and GLP-V enhanced, and both of them moved towards green and blue, compared with GLP. Both H_2O_2 and Vc have an effect on the color of polysaccharide. It may be that they forced the glyosidic bond to break, changed the structure of the sugar chain, and present different physical properties. Moreover, △E value of GLP, GLP-HV, GLP-H, and GLP-V were 36.66, 48.54, 45.29, and 47.78, respectively. These three degradation methods had influence on the color brightness, yellowness and redness of polysaccharide. Degradation heightened the brightness of polysaccharide and improved its color.

3.4. XRD determination

The XRD analysis was carried out to evaluate the structural modifications and the molecular conformation changes caused by degradation. As shown in Fig. 1, the XRD curve of two broad peaks at $2\theta = 19^\circ$ and 25.5° were observed in GLP. The peaks area were blunt and wide, indicating that GLP had amorphous polymer structure with poor crystallinity (Bozoglan, Duman, & Tunc, 2020). After degradation by H_2O_2 or Vc, the intensity of the first peak were enhanced which illustrating the augment of crystal structure. However, the peak of GLP-HV at 19° (2θ) changed sharper with larger height and area, comparing to GLP, GLP-H, and GLP-V. In the meanwhile, some little sharp peaks were observed in GLP-HV at $2\theta = 15^\circ$, 30.2°, and 32.2°. These results demonstrated that polysaccharide have the microcrystalline structure after degradation. The results were in line with Wang et al. (2021). Moreover, H_2O_2, Vc and H_2O_2-Vc were able to affect the crystal structure of polysaccharide, promoting its crystallinity. It may be that free radicals attacked the glyosidic bond, which made polysaccharide structure more uniform and its crystallinity increased. The impact of H_2O_2 combined with Vc was more effective than any of them, showing that Vc promoted the amount of free radical produced by H_2O_2.

3.5. Thermal stability analysis

TG, DTG and DSC were performed to determine the effect of degradation on thermal stability of polysaccharide and its degradation products at a range of 30–900 ∘C (as seen in Fig. 2). In the TG curve, the first

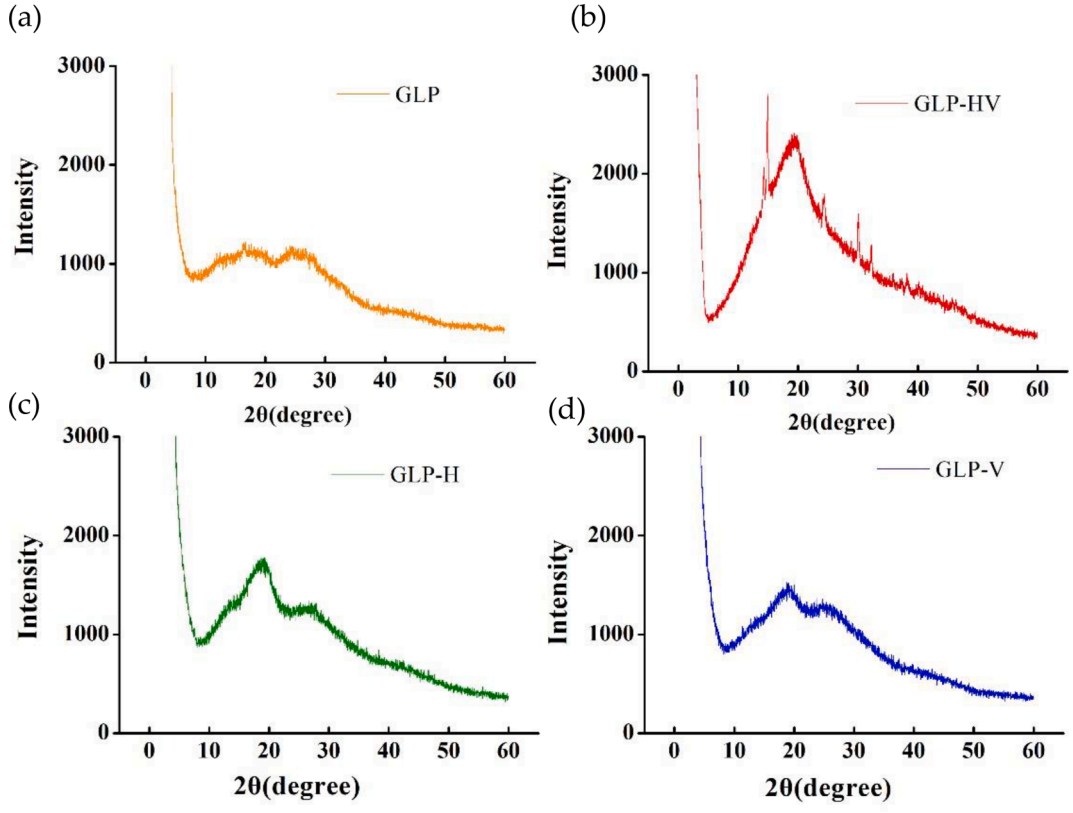

Fig 1. The XRD analysis of *Gracilaria lemaneiformis* polysaccharide and its degradation products.

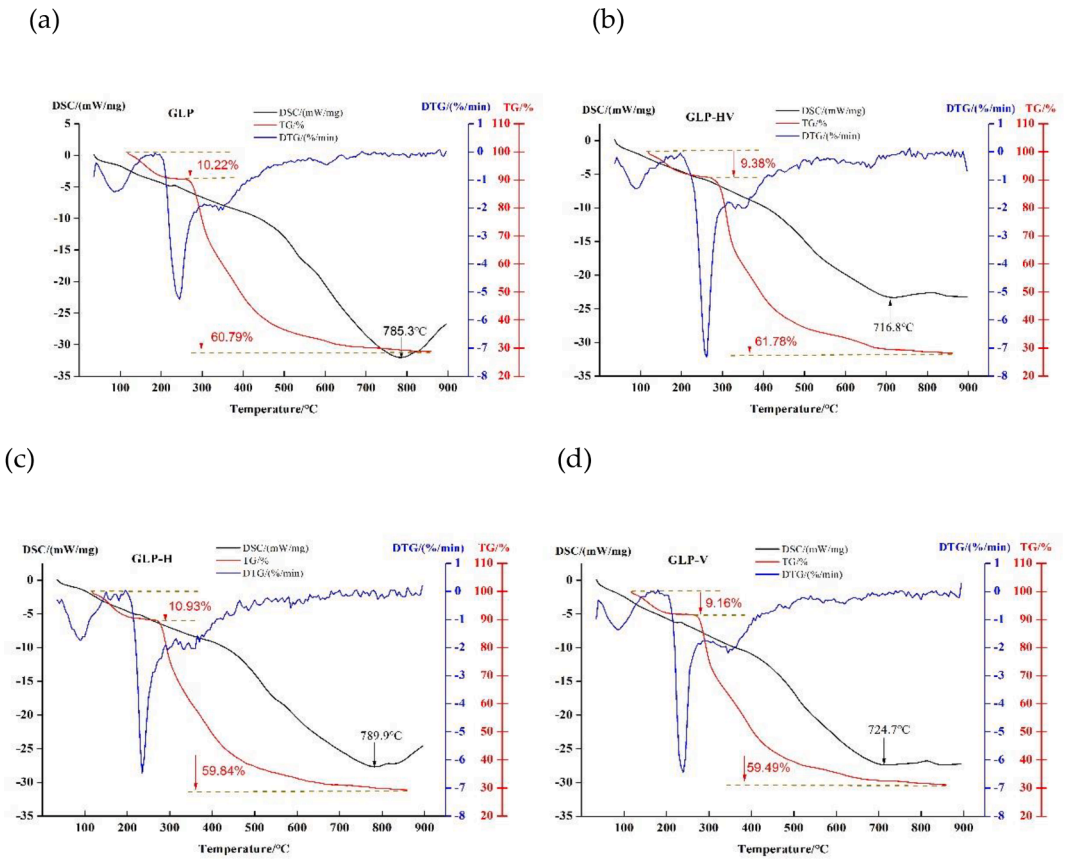

Fig. 2. Thermal stability analysis of *Gracilaria lemaneiformis* polysaccharide and its degradation products.

thermal event was observed from 35 to 120 ∘C that the mass loss of GLP (10.22%), GLP-HV (9.38%), GLP-H (10.93%), and GLP-V (9.16%), were attributed to the loss of the adsorbed water, bound water and crystallization water. And the main decomposition step occurred at 210–500 ∘C, this step was related to the breakage of the glyosidic bond (Tang et al., 2021). The mass loss rate of polysaccharides before and after degradation were after the polysaccharide was degraded by H_2O_2-Vc, as also close at this step. The results in this research were similar to the Chen et al. (2020), who studied the thermal stability analysis of GLP extracted by various methods.

DTG curve area is the curve obtained by the first derivative of TG curve to temperature (or time), representing the relationship between mass loss rate and temperature (or time). The curve area is proportional to mass loss. As can be seen from the DTG curve, decomposition was mainly divided into two processes, and the area of the two peaks did not change significantly before and after degradation of polysaccharide. Both TG and DTG curve illustrated that there was no significant change in thermal stability of polysaccharide before and after degradation. This indicated that the thermal stability of polysaccharide had little relation with the structure of sugar chain.

The differential scanning calorimetry (DSC) curve represents the rate of heat absorption or release of the sample, and the area surrounded by peaks or valleys in the curve reflects the change of heat, so DSC can directly measure the thermal effect of the sample in physical or chemical changes (Iijima, Hatakeyama, & Hatakeyama, 2012). The endothermic peaks of GLP, GLP-HV, GLP-H and GLP-V appeared at 785.3, 716.8, 789.9 and 724.7 ℃, respectively, indicating the transformation of solid configuration of polysaccharide and its degradation products, and the phase structure did not change before and after degradation. However, it may be that the hydrogen and glyosidic bonds between molecules were diverse due to degradation, resulting in slight differences in the temperature and rate of the endothermic peak of the degraded polysaccharide.

3.6. AFM analysis

Atomic force microscopy (AFM) is an effective method to observe the surface morphology of polysaccharide, which can be used for visualization and functional analysis of biological macromolecules (Gong et al., 2021). The AFM analysis of polysaccharide and its degradation products occurred in Fig. 3, including two-dimensional map 2D and three-dimensional map 3D. As represented in Fig. 3(a), the distribution of GLP was not uniform, the size was heterogeneous, and most particles were aggregated. The height of GLP ranged from −2.0 nm to 7.2 nm, while GLP-HV was from −608.0 pm to 1.5 nm (Fig. 3(b)), lower than GLP. Moreover, polysaccharide changed to delicacy and dispersion treated by H_2O_2-Vc. Fig. 3(c) and (d) displayed a few parts of aggregation in the GLP-H (height of −1.0 nm to 2.7 nm) and GLP-V (height of −1.2 nm to 4.0 nm). The value of "Image Ra" were 0.547, 0.207, 0.322, and 0.345 nm of GLP, GLP-HV, GLP-H and GLP-V, calculated by the software of NanoScope Analysis 1.8, which demonstrated the roughness was declined after degradation. The height, roughness and distribution of polysaccharide particles were affected by H_2O_2 or Vc, and H_2O_2 combined with Vc played the obvious effect, which may related to the breakage of glyosidic bonds. The result was consistent with the particle size. And the results were also similar to Yan et al. (2021), polysaccharide showed the smaller height and better uniformity. Moreover, the morphology and aggregation degree of polysaccharide may affect the color and activity of polysaccharides. The accumulation of polysaccharide may make it darker. In addition, the dispersion of sample may prove the interaction area between polysaccharide molecules, thus affecting its activity.

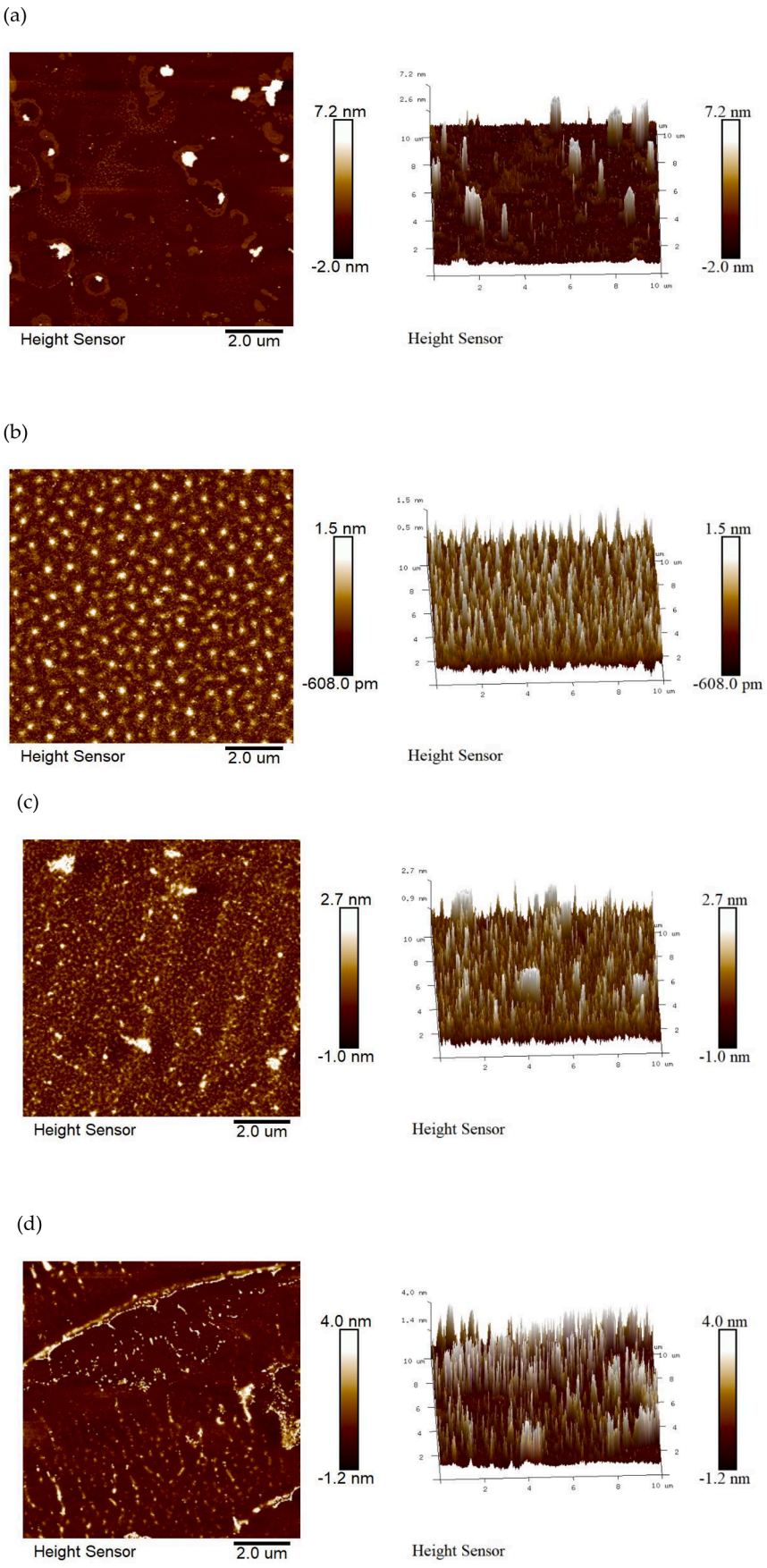

Fig. 3. AFM analysis of *Gracilaria lemaneiformis* polysaccharide and its degradation products.

3.7. FT-IR analysis

The FT-IR spectrum of GLP, GLP-HV, GLP-H and GLP-V were displayed in Fig. 4. All of these four samples exhibited a typical strong and wide peak around 3421 cm^{-1} due to O—H stretching vibration (Wen, Zhang, Sun-Waterhouse, You, & Fu, 2017), and the degradations presented a little stronger absorption, especially. Stretching band appeared at 2353 cm^{-1} may due to the stretching vibration of O═C═O. The signal at 2929 cm^{-1} corresponded to bending vibration of C—H (Wen et al., 2017). Stretching bands appeared at 1647 cm^{-1} was connected with stretching vibration of N—H—C—O, which may result from the bound water (Liao, Yang, Chen, Yu, Zhang & Ju, 2015). GLP was observed the vibration of deprotonated carboxylic group at 1550 cm^{-1} (Han et al., 2020), while the degradation products manifested the stronger signal at this peak, declaring the enhance of carboxylic group after treated by H_2O_2-Vc. Stretching bands were observed at 1408 cm^{-1}, 1371 cm^{-1} and 1242 cm^{-1} that possibly ascribed to ester sulfate groups, indicating the presence of sulfate groups (Chen et al., 2020; Chen et al., 2010; Li et al., 2020). The strong band distribution of 1200–950 cm^{-1} is specific region to polysaccharides, expounding the possible characteristics of polysaccharide according to the position and intensity of the spectrum. Both the absorption peaks at 1153 cm^{-1} and 773 cm^{-1} were caused by vibrations of α-glyosidic bonds (Gong et al., 2021; Li et al., 2020; Wu, Lu, & Wang, 2017). The sharp peak at 1070 cm^{-1} was assigned to stretching vibration of glyosidic linkage C—O—H. Weak absorptions at 935 and 887 cm^{-1} due to C—O vibration of 3,6-anhydro-L-galactose and β-D-glucopyranose, revealing the existence of 3,6-anhydro-L-galactose and glucose (Chen et al, 2010; Fan et al, 2012; Liao et al., 2015). FT-IR spectrum analysis revealed that the strength of carbonyl group and sulfate group enhanced after degradation, which may be related to the breakage of glyosidic bonds of polysaccharide via free radicals produced by H_2O_2 and Vc. These results displayed that polysaccharide and its degradation products were the typical sulfated polysaccharide, accompanied with 3,6-anhydro-L-galactose. Moreover, H_2O_2-Vc degradation never produced new groups, nor eliminated functional groups of polysaccharide.

3.8. The inhibition effect on pancreatic lipase

Recent studies have demonstrated that pancreatic lipase is a key enzyme in the digestion and absorption of fat in the intestinal tract, which can hydrolyze 50%–70% dietary fat and convert it into glycerol monoesters and fatty acids in human body (Siegien et al., 2021; Yuan, Xu, Jing, Zou, Zhang, & Li 2018). The effect of inhibitor on pancreatic lipase activity intercepts the production of glycerol monoesters and fatty acids thereby enhancing the hypolipidemic activity. This kind of inhibition effect is mainly reflected by inhibition rate, IC_{50} value, inhibition kinetics and fluorescence quenching. In addition, orlistat inhibits lipase in the gastrointestinal tract, prevents hydrolysis of triacylglycerol to free fatty acids and monoacylglycerol, reduces absorption of dietary fat by intestinal mucosa, and promotes fat elimination from the body. However, orlistat with prolonged use makes gastric bowel exhaust increase, occurrence defecate urgent feeling, adipose sex defecate and adipose diarrhoea wait for a circumstance (Li et al., 2021). As algal polysaccharide, GLP should have higher safety. Therefore, the hypolipidemic activity of polysaccharide *in vitro* was investigated by measuring the inhibitory activity of polysaccharide on pancreatic lipase. Considering the effective inhibition of orlistat, we chose it to be positive control.

Fig. 5 presented the inhibition effect of GLP and its degradation products on pancreatic lipase. In Fig. 5(a), all of these four samples expressed certain inhibitory effect on pancreatic lipase at the content of 1 to 10 mg/mL. In this concentration range, three degraded polysaccharide exhibited dose-dependent, while the inhibition rate of GLP declined at 7.5 mg/mL. This may be related to the viscosity of GLP, which was enhanced with increasing concentration, and high viscosity of polysaccharide may limit its inhibitory activity on lipase decrease. Moreover, it was also possible that the inhibitory effect of GLP on lipase had reached saturation at the concentration of 7.5 mg/mL, and the inhibitory effect will be weakened exceeds 7.5 mg/mL. GLP-HV presented the best inhibition action, next was GLP-V, while GLP and GLP-H performed a similar effect. It pointed out that H_2O_2-Vc degraded polysaccharide produced the lower molecular weight polysaccharide with excellent hypolipidemic activity *in vitro*. The IC_{50} of GLP, GLP-HV, GLP-

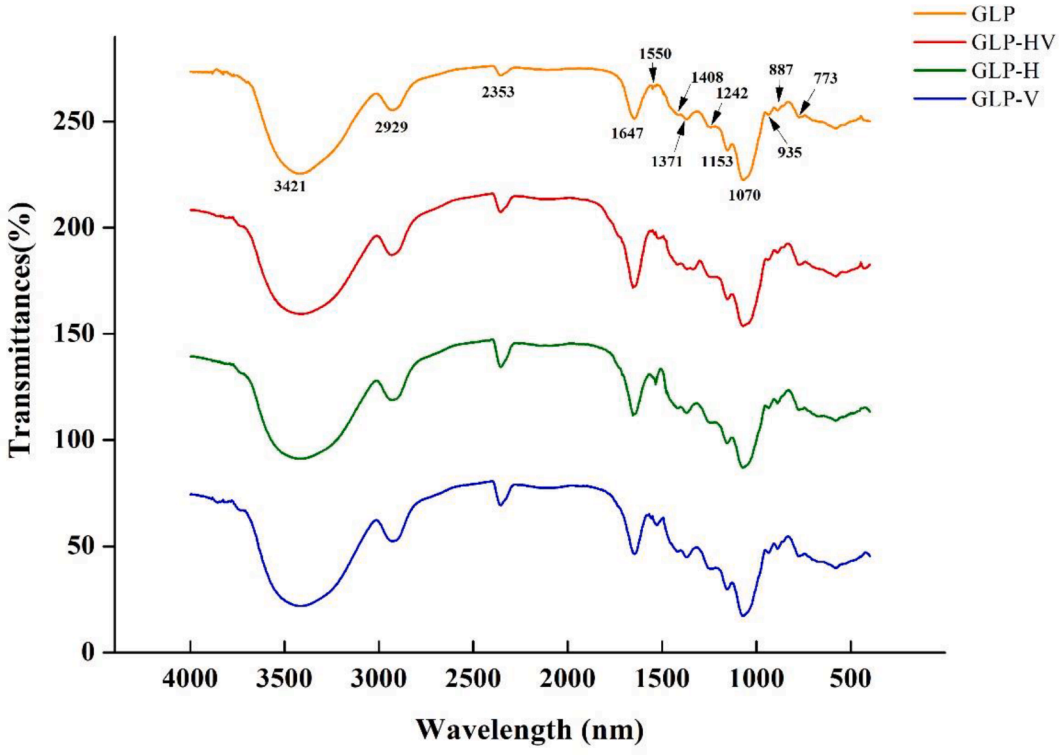

Fig. 4. FT-IR analysis of *Gracilaria lemaneiformis* polysaccharide and its degradation products.

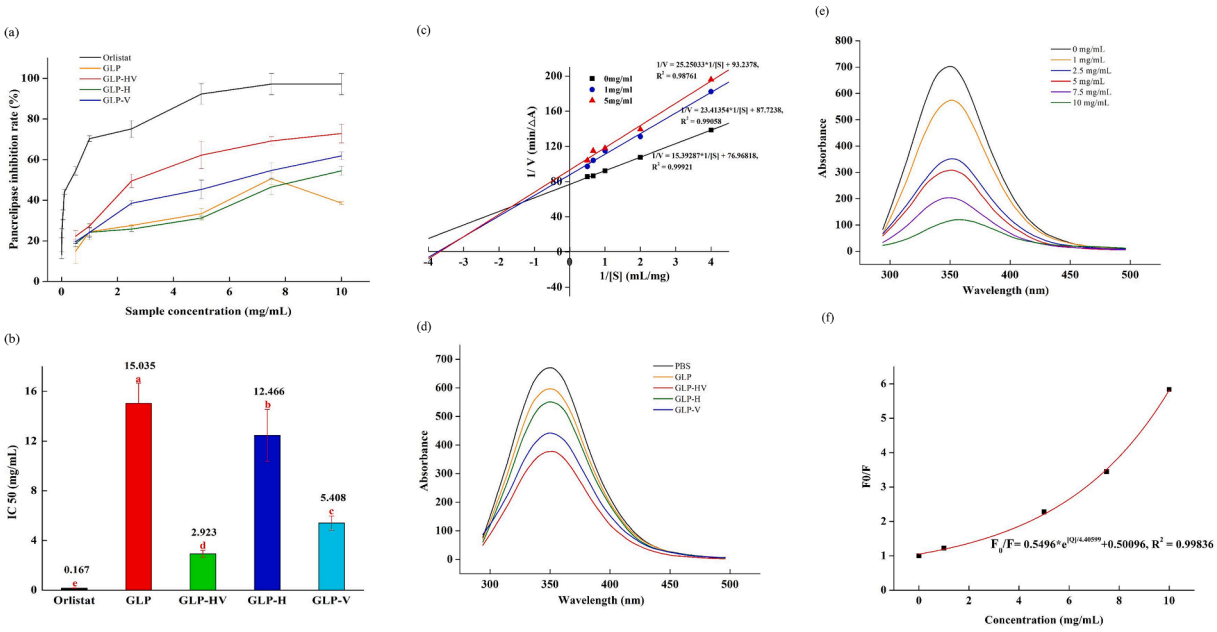

Fig. 5. The inhibition effect of *Gracilaria lemaneiformis* polysaccharide and its degradation products on pancreatic lipase. Note: (a) The pancreatic lipase inhibition rate of GLP, GLP-HV, GLP-H, and GLP-V; (b) The IC_{50} value of pancreatic lipase inhibition rate of GLP, GLP-HV, GLP-H, and GLP-V; (c) The *Lineweaver–Burk* curve of pancreatic lipase inhibitory dynamics of GLP, GLP-HV, GLP-H, and GLP-V; (d) The fluorescence spectrum analysis on pancreatic lipase of GLP, GLP-HV, GLP-H, and GLP-V; (e) The fluorescence spectrum analysis on pancreatic lipase of GLP-HV; (f) The *Stern-Volmer* curve for fluorescence quenching of GLP-HV on pancreatic lipase; a, b, c and d represented significant differences among groups, and $p < 0.05$ indicates significant differences.

H, GLP-V were 15.035 ± 1.636, 2.923 ± 0.279, 12.466 ± 2.093, 5.408 ± 0.575 mg/mL, which were higher than orlistat (0.167 ± 0.013 mg/mL) (Fig. 5b). Therefore, the inhibitory effect were orlistat, GLP -HV, GLP-V, GLP-H and GLP in descending order.

GLP-HV played the best inhibition effect on pancreatic lipase that we chose GLP-HV with various concentration to evaluate its inhibition type. The *Lineweaver-Burk* curve of different concentrations of GLP-HV intersected in the second quadrant, and the slope and intercept became steepen as the concentration increased. The inhibition constants were computed and presented in Table 3 that the *Vmax* were 0.0130, 0.114, 0.0107 mg/mL·min^{-1}, and *K*m were 0.2000, 0.2669, 0.2708 mg/mL as the content of GLP-HV were 0, 1, 5 mg/mL, respectively. The value of *Vmax* decreased and *K*m enhanced, which proved the mix of competitive and non-competitive inhibition type of GLP-HV on pancreatic lipase. GLP-HV may bind to the active sites of the pancreatic lipase or affect the products formed by the pancreatic lipase and PNPB, thus achieving the inhibitory effect.

The addition of macromolecules to alter the microscopic configuration of the enzyme molecule promoted the exposure of phenylalanine (Phe), tyrosine, (Tyr) and tryptophan (Trp) residues that were previously surrounded by other amino acid residues (Zhang et al., 2019). Polysaccharide changed the microenvironment of lipase, leading to variation of quantum yield and fluorescence intensity, and the degree of this change was related to the degradation methods and concentration of polysaccharide. As presented in Fig. 5d, GLP-HV performed the strongest effect on fluorescence intensity, and GLP play the least trend in fluorescence intensity. On this basis, the impact of various concentrations (0, 1, 2.5, 5, 7.5, 10 mg/mL) from GLP-HV on fluorescence intensity was studied, and the results were observed in Fig. 5e, the fluorescence intensity of pancreatic lipase was lessened with the reinforce of polysaccharide concentration, which may was concerned with the amount of monosaccharides and functional groups. Calculating by fluorescence quenching *Stern-Volmer* equation, the fluorescence parameters on pancreatic lipase of GLP-HV were exhibited in Table 4 and Fig. 5f, the value of F_0/F was higher with the increase of GLP-HV concentration, suggesting the greater concentration resulting in the smaller fluorescence intensity. The quenching constant K_{sv} and K_q were 0.2270 mL/mg and 2.27 × 10^7 mL/mg/s, respectively. K_q was the maximum collision rate constant of quenchers caused by large biomolecules (Li et al., 2021). In addition, the quenching curve was presented as an exponential type cure drawn by F_0/F and [Q](Fig. 5f), revealing the static fluorescence quenching. *Ka* is the binding constant of GLP-HV with pancreatic lipase, implying the ability of degraded polysaccharide to bind to enzyme. And the value of n is on behalf of the binding sites of GLP-HV to pancreatic lipase. As illustrated in the Table 4, the value of *Ka* and n were 4.84 mL/mg and 1.27 (approached to 1), which explained the lower binding ability of GLP-HV with pancreatic lipase, and they only contained one binding site. These findings declared that all of the samples performed the excellent effect for fluorescence quenching on pancreatic lipase, and GLP-HV had the best effect, probably because GLP-HV owned the lower molecular weight and the diverse monosaccharide composition. The fluorescence quenching constants were not high, but GLP-HV played a great influence on fluorescence intensity, which might be due to the partial combination of GLP-HV and pancreatic lipase, which changed the environment around the enzyme and affected the structure of luminescent groups, thus leading to changes in fluorescence intensity.

3.9. Inhibitory effect on cholesterol esterase.

Cholesterol esterase is a special hydrolase that catalyzes the hydrolysis of cholesterol esters. It is synthesized in pancreatic acinar cells, stored in proenzyme granules, secreted into the small intestine as part of pancreatic juice, and is involved in the digestion and absorption of cholesterol in the human body. The hydrolysis of cholesterol esters to free cholesterol is an essential stage in the process of cholesterol absorption (Zhao, Wu, & Hu, 2021). Specifically, cholesterol esterase catalyzes the hydrolysis of cholesterol esters in the lumen of the small intestine, releasing free cholesterol and fatty acids to absorb by small intestinal cells. Therefore, inhibiting the activity of cholesterol esterase can effectively control the hydrolysis of cholesterol ester, and then reduce the absorption of food cholesterol by the human body, but also provides an effective way for the treatment of hyperlipidemia (Godard et al., 2009; Yasutake et al., 2021).

The inhibition rate of polysaccharide and its degradation products occurred in Fig. 6a. GLP displayed the inhibiting ability on cholesterol esterase, and the effect was remarkably improved after degradation by H_2O_2 or Vc. Polysaccharide produced by H_2O_2-Vc performed the best inhibition effect. In the range of 1 to 10 mg/ml, these four polysaccharide samples displayed remarkable inhibitory activity on cholesterol esterase in a dose-dependent manner. At a concentration of 10 mg/ml, the inhibition rate of GLP, GLP-HV, GLP-H, GLP-V were 44.53% ± 2.956, 58.47% ± 2.445, 51.80% ± 2.169, 54.63% ± 7.007, respectively. As shown in Fig. 6b, the IC_{50} values were 0.175 ± 0.008, 11.550 ± 1.089, 5.808 ± 0.457, 8.670 ± 0.826, 7.961 ± 0.531 mg/mL from olistat, GLP, GLP-HV, GLP-H, GLP-V, respectively. It proved that GLP-HV exhibited the best inhibition action on cholesterol esterase, and GLP-HV had the better action on pancreatic lipase (IC_{50} was 2.923 ± 0.279 mg/mL) than cholesterol esterase.

Lineweaver-Burk curve was plotted in Fig. 6c, which revealed the intersections of the different concentrations of GLP-HV were in the first and second quadrants. The Michaelis constant of *Km* and *Vmax* were expressed in Table 5, calculated by *Lineweaver-Burk* curve. In Table 5, *Vmax* were 0.8557, 0.4223, 0.2734 mg/mL·min^{-1}, and *Km* was 0.4801 mg/mL, with concentration of 0, 1, 5 mg/mL, severally, implying that *Vmax* declined and *Km* remained unchanged with the increase of sample content. These results confirmed that the inhibition type of GLP-HV on cholesterol esterase was non-competitive. It explained that GLP-HV combined with the inactive groups of cholesterol esterase, which did not affect the activity of the cholesterol esterase, nor did it change the intermediate products formed by the cholesterol esterase and the PNPB, but GLP-HV-cholesterol esterase-PNPB never released the products further, so as to achieve inhibition. The results were agreement with literature (Zhang, Wu, Wei, & Qin, 2020).

Phe, Tyr and Trp with endogenous fluorescence, displayed the maximum fluorescence peak at excitation wavelength of 280 nm and emission wavelength of 340 nm, respectively (Li et al., 2021). Moreover, the intensity and location of the fluorescence produced by these luminescent amino acids are closely related to their environment (Huang et al., 2020). Compared to the fluorescence intensity of pancreatic lipase and cholesterol esterase without samples, it was found that the fluorescence intensity of pancreatic lipase was stronger (Fig. 5d and Fig. 6d),

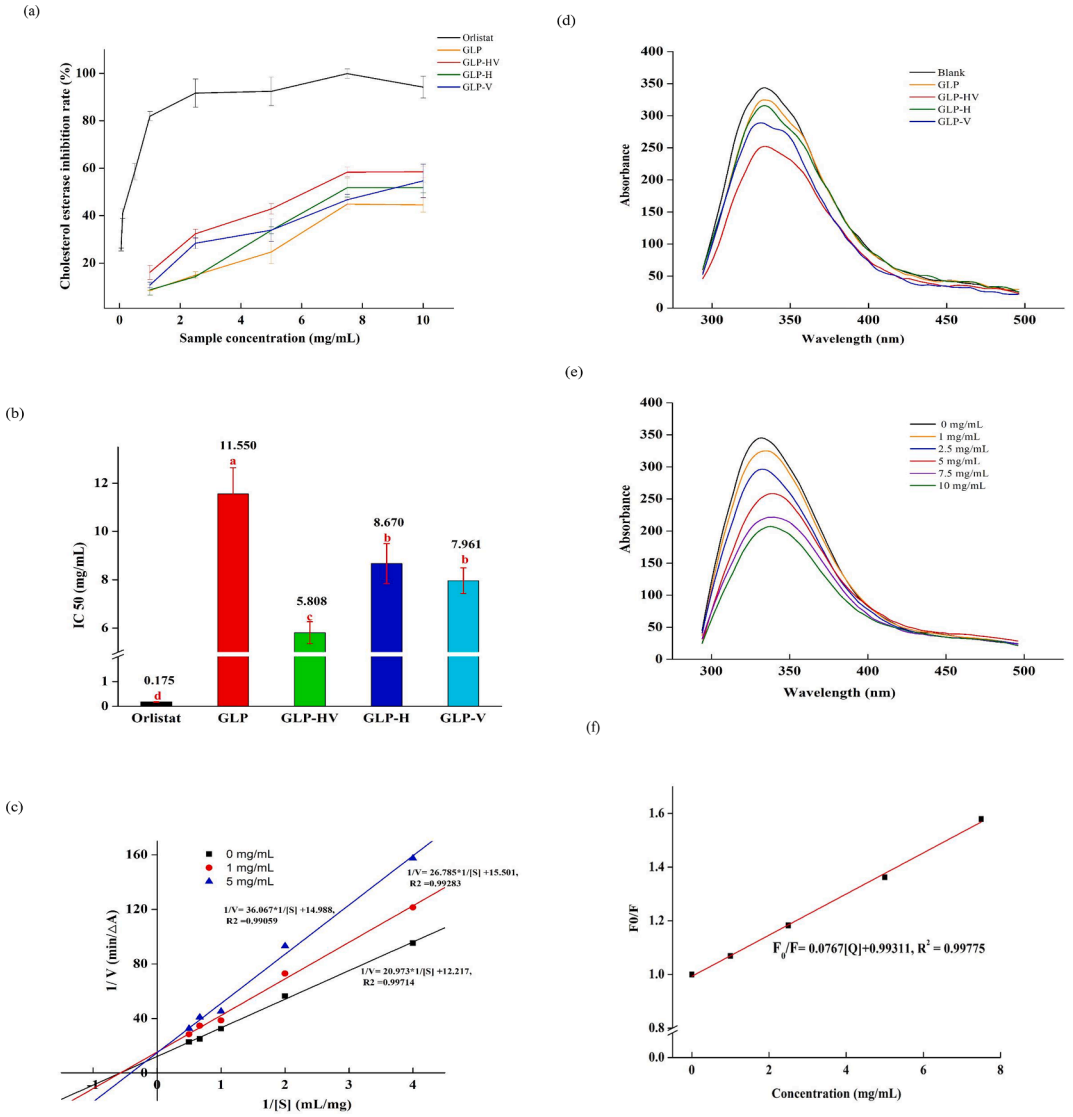

Fig. 6. The inhibition effect of *Gracilaria lemaneiformis* polysaccharide and its degradation products on cholesterol esterase. Note: (a) The cholesterol esterase inhibition rate of GLP, GLP-HV, GLP-H, and GLP-V; (b) The IC_{50} value of cholesterol esterase inhibition rate of GLP, GLP-HV, GLP-H, and GLP-V; (c) The *Lineweaver–Burk* curve of cholesterol esterase inhibitory dynamics of GLP, GLP-HV, GLP-H, and GLP-V; (d) The fluorescence spectrum analysis on cholesterol esterase of GLP, GLP-HV, GLP-H, and GLP-V; (e) The fluorescence spectrum analysis on pancreatic lipase of GLP-HV; (f) The *Stern-Volmer* curve for fluorescence quenching of GLP-HV on cholesterol esterase; a, b, c and d represented significant differences among groups, and $p < 0.05$ indicates significant differences.

which was caused by its luminescent amino acids and their surroundings. As exhibited in Fig. 6d, all of the samples performed fluorescence quenching to some extent, and GLP-HV still presented the best function on cholesterol esterase, similar to pancreatic lipase. Therefore, the effect of GLP-HV with various concentrations on fluorescence quenching was investigated. The fluorescence quenching and its parameters on cholesterol esterase were shown in Fig. 6e, 6f and Table 6. As presented in Fig. 6e, the concentration of GLP-HV exhibited a significant role in fluorescence quenching of cholesterol esterase, and the higher concentration could cause the stronger quenching function, like the result of pancreatic lipase. However, the valve of F_0/F from cholesterol esterase was smaller than pancreatic lipase at the same concentration, illustrating the stronger red shift occurred in pancreatic lipase so that expressed the best fluorescence quenching of GLP-HV on pancreatic lipase than cholesterol esterase. Moreover, the quenching constant *Ksv* and *Kq* were 0.0767 mL/mg and 7.67 $\times$ 10^6 mL/mg/s, respectively, which were lower than pancreatic lipase. It also demonstrated that GLP-HV emerged the better fluorescence quenching on pancreatic lipase than cholesterol esterase. The fluorescence quenching curve was almost straight line in Fig. 6f that the fluorescence quenching type may be dynamic quenching. On the other hand, the binding constant was 14.45 mL/mg, bigger than pancreatic lipase, and binding site was 1.0456 (also approximately equal to 1). GLP-HV potentially manifested the stronger combination ability to cholesterol esterase, but the different locations of bind sites or the less effect on the luminescent groups environment resulted in the weaker fluorescence quenching on cholesterol esterase than pancreatic lipase.

GLP-HV played the best inhibition on pancreatic lipase and cholesterol esterase than GLP, which may related with the lower molecular weight, smaller particle size, higher carbonyl group and sulfate group, and crystal structure. H_2O_2-Vc degradation promoted the rupture of glyosidic bonds, shortening of sugar chains, reduction of average molecular particle size, and enhanced the intermolecular interaction area among molecules. Moreover, the content of carbonyl and sulfate groups increased, which reinforced the inhibition of polysaccharides on pancreatic lipase and cholesterol esterase.

4. Conclusion

The content of galacturonic acid declined and glucuronic acid level enhanced, average particle size decreased, and color brightness of polysaccharide strengthened degraded by H_2O_2-Vc. XRD proved the microcrystalline structure of GLP-HV with a sharp peak at $2\theta = 19°$, and there was no significant change in thermal stability after degradation. Polysaccharide changed to smaller, delicacy and dispersion after degradation from AFM analysis. FT-IR demonstrated the functional groups did not change, except for carbonyl and sulfate groups which were slightly strengthened after degradation. GLP-HV showed a significant inhibition effect on pancreatic lipase and cholesterol esterase in a dose-dependent manner, which presented the mixed type of competitive and non-competitive for pancreatic lipase, and non-competitive for cholesterol esterase, respectively. The fluorescence quenching type was static on pancreatic lipase and dynamic on cholesterol esterase. GLP-HV played an important role in hypolipidemic activity *in vitro*, which may related to the contents of uronic acid, sulfate group, carbonyl group, microstructure and the connection of glyosidic bond.

Funding

This work was supported by the Key-Area Research and Development Program of Guangdong Province (2020B1111030004), the National Key R&D Program of China (2019YFD0901905), the China Agriculture Research System of MOF and MARA (CARS-50), the Special Scientific Research Funds for Central Non-profit Institutes, Chinese Academy of Fishery Sciences (2020TD69), the Central Public-interest Scientific Institution Basal Research Funds, South China Sea Fisheries Research Institute, CAFS (2021SD06), and the Pearl River S&T Nova Program of Guangzhou (201906010081).

CRediT authorship contribution statement

Xiaoshan Long: Data curation, Writing – original draft. **Xiao Hu:** Funding acquisition, Project administration, Writing – review & editing. **Huan Xiang:** Formal analysis. **Shengjun Chen:** Investigation, Software. **Laihao Li:** Funding acquisition, Methodology, Resources. **Bo Qi:** Formal analysis. **Chunsheng Li:** Methodology. **Shucheng Liu:** Supervision, Validation, Writing – review & editing. **Xianqing Yang:** Funding acquisition, Project administration, Resources, Visualization, Writing – review & editing.

Declaration of Competing Interest

The authors declare that they have no known competing financial interests or personal relationships that could have appeared to influence the work reported in this paper.

Appendix A. Supplementary data

Supplementary data to this article can be found online at https://doi.org/10.1016/j.fochx.2022.100314.

References

Aggarwal, V., Malik, J., Prashant, A., Jaiwal, P. K., & Pundir, C. S. (2016). Amperometric determination of serum total cholesterol with nanoparticles of cholesterol esterase and cholesterol oxidase. *Analytical Biochemistry, 500*, 6–11.

Bendiak, B., Salyan, M. E., & Pantoja, M. (1994). Sequential removal of monosaccharides from the reducing end of oligosaccharides. I. A reaction between hydrazine and sugars having a glycosidic substituent on a carbon atom adjacent to the carbonyl group. *Tetrahedron Letters, 35*(5), 685–688. https://doi.org/10.1016/s0040-4039(00)75790-x

Bettler, B., Amadò, R., & Neukom, H. (1990). Electrophoresis of uronic acids, neutral sugars and hydrolysates of acidic polysaccharides on silylated glass-fibre paper in electrolytes of bivalent cations. *Journal of Chromatography A, 498*, 223–230. https://doi.org/10.1016/s0021-9673(01)84250-3

Boyd, A. P., Talbert, J. N., & Acevedo, N. C. (2021). Effect of agitation and added cholesterol esterase on bioaccessibility of phytosterols in a standardized in vitro digestion model. *Lwt, 150*, Article 112051.

Bozoglan, B. K., Duman, O., & Tunc, S. (2020). Preparation and characterization of thermosensitive chitosan/carboxymethylcellulose/scleroglucan nanocomposite hydrogels. *International Journal of Biological Macromolecules, 162*, 781–797.

Chen, H. J., Xiao, Q., Weng, H. F., Zhang, Y. H., Yang, Q. M., & Xiao, A. F. (2020). Extraction of sulfated agar from Gracilaria lemaneiformis using hydrogen peroxide-assisted enzymatic method. *Carbohydrate Polymers, 232*, Article 115790.

Chen, M. Z., Xie, H. G., Yang, L. W., Liao, Z. H., & Yu, J. (2010). In vitro anti-influenza virus activities of sulfated polysaccharide fractions from Gracilaria lemaneiformis. *Virologica Sinica, 25*(5), 341–351.

Chen, S., Liu, H., Yang, X., Li, L., Qi, B., Hu, X., … Pan, C. (2020). Degradation of sulphated polysaccharides from Grateloupia livida and antioxidant activity of the degraded components. *International Journal of Biological Macromolecules, 156*, 660–668.

Chen, X., Li, X., Sun-Waterhouse, D., Zhu, B., You, L., & Hileuskaya, K. (2021). Polysaccharides from Sargassum fusiforme after UV/H2O2 degradation effectively ameliorate dextran sulfate sodium-induced colitis. *Food & Function, 12*(23), 11747–11759.

Fan, Y. L., Wang, W. H., Song, W., Chen, H. S., Teng, A. G., & Liu, A. J. (2012). Partial characterization and anti-tumor activity of an acidic polysaccharide from Gracilaria lemaneiformis. *Carbohydrate Polymers, 88*(4), 1313–1318.

Godard, M., Décordé, K., Ventura, E., Soteras, G., Baccou, J. C., Cristol, J. P., & Rouanet, J. M. (2009). Polysaccharides from the green alga Ulva rigida improve the antioxidant status and prevent fatty streak lesions in the high cholesterol fed hamster, an animal model of nutritionally-induced atherosclerosis. *Food Chemistry, 115*(1), 176–180.

Gong, Y., Ma, Y., Cheung, P. C., You, L., Liao, L., Pedisic, S., & Kulikouskaya, V. (2021). Structural characteristics and anti-inflammatory activity of UV/H2O2-treated algal sulfated polysaccharide from Gracilaria lemaneiformis. *Food and Chemical Toxicology, 152*, Article 112157.

Han, R., Wang, L., Zhao, Z. G., You, L. J., Pedisic, S., Kulikouskaya, V., & Lin, Z. Q. (2020). Polysaccharide from Gracilaria Lemaneiformis prevents colitis in Balb/c mice via enhancing intestinal barrier function and attenuating intestinal inflammation. *Food Hydrocolloids, 109*, Article 106048.

Heng, S., Tieu, W., Hautmann, S., Kuan, K., Pedersen, D. S., Pietsch, M., … Abell, A. D. (2011). New cholesterol esterase inhibitors based on rhodanine and thiazolidinedione scaffolds. *Bioorganic & Medicinal Chemistry, 19*(24), 7453–7463.

Huang, S. M., Pang, D. R., Li, X., You, L. J., Zhao, Z. G., Cheung, P. C. K., … Liu, D. (2019). A sulfated polysaccharide from Gracilaria Lemaneiformis regulates cholesterol and bile acid metabolism in high-fat diet mice. *Food & Function, 10*(6), 3224–3236.

Huang, X., Zhu, J., Wang, L., Jing, H., Ma, C., Kou, X., & Wang, H. (2020). Inhibitory mechanisms and interaction of tangeretin, 5-demethyltangeretin, nobiletin, and 5-demethylnobiletin from citrus peels on pancreatic lipase: Kinetics, spectroscopies, and molecular dynamics simulation. *International Journal of Biological Macromolecules, 164*, 1927–1938.

Iijima, M., Hatakeyama, T., & Hatakeyama, H. (2012). DSC and TMA studies on freezing and thawing gelation of galactomannan polysaccharide. *Thermochimica Acta, 532*, 83–87.

Li, R., Xue, Z., Jia, Y., Wang, Y., Li, S., Zhou, J., … Chen, H. (2021). Polysaccharides from mulberry (Morus alba L.) leaf prevents obesity by inhibiting pancreatic lipase in high-fat diet induced mice. *International Journal of Biological Macromolecules, 192*, 452–460.

Li, X., Huang, S., Chen, X., Xu, Q., Ma, Y., You, L., … Piao, J. (2020). Structural characteristic of a sulfated polysaccharide from Gracilaria Lemaneiformis and its lipid metabolism regulation effect. *Food & Function, 11*(12), 10876–10885.

Liao, X., Yang, L., Chen, M., Yu, J., Zhang, S., & Ju, Y. (2015). The hypoglycemic effect of a polysaccharide (GLP) from Gracilaria lemaneiformis and its degradation products in diabetic mice. *Food & Function, 6*(8), 2542–2549.

Long, X. S., Hu, X., Liu, S. C., Pan, C., Chen, S. J., Li, L. H., … Yang, X. Q. (2021a). Insights on preparation, structure and activities of Gracilaria lemaneiformis polysaccharide. *Food Chemistry X, 12*, Article 100153.

Long, X. S., Hu, X., Zhou, S. B., Xiang, H., Chen, S. J., Li, L. H., … Yang, X. Q. (2021b). Optimized degradation and inhibition of α-glucosidase activity by Gracilaria lemaneiformis polysaccharide and its production in vitro. *Marine Drugs, 20*(1), 13.

Nawrocka, A., Chargot, M. S., Miś, A., Wilczewska, A. Z., & Markiewicz, K. H. (2017). Effect of dietary fibre polysaccharides on structure and thermal properties of gluten proteins – A study on gluten dough with application of FT-Raman spectroscopy, TGA and DSC. *Food Hydrocolloids, 69*, 410–421.

Shen, X., Liu, Z., Li, J., Wu, D., Zhu, M., Yan, L., … Chen, S. (2019). Development of low molecular weight heparin by H2O2/ascorbic acid with ultrasonic power and its anti-metastasis property. *International Journal of Biological Macromolecules, 133*, 101–109.

Siegien, J., Buchholz, T., Popowski, D., Granica, S., Osinska, E., Melzig, M. F., & Czerwinska, M. E. (2021). Pancreatic lipase and alpha-amylase inhibitory activity of extracts from selected plant materials after gastrointestinal digestion in vitro. *Food Chemistry, 355*, Article 129414.

Singh, S., Chaubey, A., & Malhotra, B. D. (2004). Amperometric cholesterol biosensor based on immobilized cholesterol esterase and cholesterol oxidase on conducting polypyrrole films. *Analytica Chimica Acta, 502*(2), 229–234.

Siow, H.-L., Choi, S.-B., & Gan, C.-Y. (2016). Structure–activity studies of protease activating, lipase inhibiting, bile acid binding and cholesterol-lowering effects of pre-screened cumin seed bioactive peptides. *Journal of Functional Foods, 27*, 600–611. https://doi.org/10.1016/j.jff.2016.10.013

Sun, X. N., Duan, M. M., Liu, Y. L., Luo, T. R., Ma, N., Song, S., & Ai, C. Q. (2018). The beneficial effects of Gracilaria lemaneiformis polysaccharides on obesity and the gut microbiota in high fat diet-fed mice. *Journal of Functional Foods, 46*, 48–56.

Tang, L., Luo, X., Wang, M., Wang, Z., Guo, J., Kong, F., & Bi, Y. (2021). Synthesis, characterization, in vitro antioxidant and hypoglycemic activities of selenium nanoparticles decorated with polysaccharides of Gracilaria lemaneiformis. *International Journal of Biological Macromolecules, 193*(Pt A), 923–932.

Wang, L., Li, L., Gao, J., Huang, J., Yang, Y., Xu, Y., … Yu, W. (2021). Characterization, antioxidant and immunomodulatory effects of selenized polysaccharides from dandelion roots. *Carbohydrate Polymers, 260*, Article 117796.

Wang, S., Li, Y., Huang, D., Chen, S., Xia, Y., & Zhu, S. (2022). The inhibitory mechanism of chlorogenic acid and its acylated derivatives on alpha-amylase and alpha-glucosidase. *Food Chemistry, 372*, Article 131334.

Wang, X. M., Zhang, Z. S., Zhou, H. C., Sun, X., Chen, X. P., & Xu, N. J. (2019). The anti-aging effects of Gracilaria lemaneiformis polysaccharide in Caenorhabditis elegans. *International Journal of Biological Macromolecules, 140*, 600–604.

Wen, L. R., Zhang, Y. L., Sun-Waterhouse, D. X., You, L. J., & Fu, X. (2017). Advantages of the polysaccharides from Gracilaria lemaneiformis over metformin in antidiabetic effects on streptozotocin-induced diabetic mice. *RSC Advances, 7*(15), 9141–9151.

Wiacek, J., & Stasiak, M. (2018). Effect of the particle size ratio on the structural properties of granular mixtures with discrete particle size distribution. *Granular Matter, 20*(2).

Wu, S. J., Lu, M. S., Wang, S. J. (2017). Amylase-assisted extraction and antioxidant activity of polysaccharides from Gracilaria lemaneiformis. *3 Biotech, 7*(1).

Yan, S. L., Pan, C., Yang, X. Q., Chen, S. J., Qi, B., & Huang, H. (2021). Degradation of Codium cylindricum polysaccharides by H2O2-Vc-ultrasonic and H2O2-Fe2+-ultrasonic treatment: Structural characterization and antioxidant activity. *International Journal of Biological Macromolecules, 182*, 129–135.

Yasutake, Y., Konishi, K., Muramatsu, S., Yoshida, K., Aburatani, S., Sakasegawa, S. I., & Tamura, T. (2021). Bacterial triacylglycerol lipase is a potential cholesterol esterase: Identification of a key determinant for sterol-binding specificity. *International Journal of Biological Macromolecules, 167*, 578–586.

Yuan, Y., Xu, X., Jing, C., Zou, P., Zhang, C., & Li, Y. (2018). Microwave assisted hydrothermal extraction of polysaccharides from Ulva prolifera: Functional properties and bioactivities. *Carbohydrate Polymers, 181*, 902–910.

Zhang, C. H., Yun, Y. H., Zhang, Z. M., & Liang, Y. Z. (2016). Simultaneous determination of neutral and uronic sugars based on UV–vis spectrometry combined with PLS. *International Journal of Biological Macromolecules, 87*, 290–294. https://doi.org/10.1016/j.ijbiomac.2016.02.066

Zhang, H. L., Wu, Q. X., Wei, X., & Qin, X. M. (2020). Pancreatic lipase and cholesterol esterase inhibitory effect of Camellia nitidissima Chi flower extracts in vitro and in vivo. *Food Bioscience, 37*, Article 100682.

Zhang, X., Aweya, J. J., Huang, Z. X., Kang, Z. Y., Bai, Z. H., Li, K. H., … Cheong, K. L. (2020). In vitro fermentation of Gracilaria lemaneiformis sulfated polysaccharides and its agaro-oligosaccharides by human fecal inocula and its impact on microbiota. *Carbohydrate Polymers, 234*, Article 115894.

Zhang, Y., Luo, X. A., Zhu, L. J., Wang, S. Z., Jia, M. Q., & Chen, Z. X. (2019). Catalytic behavior of pancreatic lipase in crowded medium for hydrolysis of medium-chain and long-chain lipid: An isothermal titration calorimetry study. *Thermochimica Acta, 672*, 70–78.

Zhang, Z., Wang, X., Zhao, M., & Qi, H. (2014). Free-radical degradation by Fe2+/Vc/H2O2 and antioxidant activity of polysaccharide from Tremella fuciformis. *Carbohydrate Polymers, 112*, 578–582.

Zhao, S., Wu, Y., & Hu, L. (2021). Identification and synthesis of selective cholesterol esterase inhibitor using dynamic combinatorial chemistry. *Bioorganic Chemistry, 119*, Article 105520.